VOL. 10, NO. 1, JAN.-FEB. 1987 J. GUIDANCE

Nonlinear Flight Test Trajectory Controllers for Aircraft

P.K.A. Menon,* M.E. Badgett,† and R.A. Walker‡
Integrated Systems, Inc., Palo Alto, California
and
E.L. Duke§
NASA Ames-Dryden Flight Research Facility, Edwards, California

Flight test trajectory control systems are designed to enable the pilot to follow complex trajectories for evaluating an aircraft within its known flight envelope and to explore the boundaries of its capabilities. Previous design approaches were based on linearized aircraft models necessitating a large amount of data storage along with gain schedules. In this paper, the synthesis of nonlinear flight test trajectory controllers for a fixed-wing aircraft is described. This approach uses singular perturbation theory and the recently developed theory of prelinearizing transformations. These controllers do not require gain scheduling for satisfactory operation, can be used in arbitrarily nonlinear maneuvers, and are mechanized with a direct, noniterative analytic solution.

Nomenclature

D	= drag
e_1, e_2, e_3	= control surface influence coefficients for moments about roll body axis X
f_1, f_2, f_3	= control surface influence coefficients for moments about pitch body axis Y
g_1, g_2, g_3	= control surface influence coefficients for moments about yaw body axis Z
H	= altitude rate
h	= altitude
I_x	= X body axis moment of inertia
I_{xy}	= X-Y body axis product of inertia
I_{xz}	= X-Z body axis product of inertia
I_y	= Y body axis moment of inertia
I_{yz}	= Y-Z body axis product of inertia
I_z	= Z body axis moment of inertia
$k_1 T$	= component of thrust along the X body axis
$k_2 T$	= component of thrust along the Y body axis
$k_3 T$	= component of thrust along the Z body axis
L	= lift
M	= Mach number
m	= aircraft mass
q	= pitch body rate
r	= yaw body rate
P	= total aerodynamic and thrust moment about the X body axis, not including the control moments
Q	= total aerodynamic and thrust moment about Y body axis, not including control moments
R	= total aerodynamic and thrust moment about Z body axis, not including control moments
S	= side force
T	= engine thrust
V	= total velocity
α	= angle of attack
β	= angle of sideslip
δ_a	= aileron deflection
δ_e	= elevator deflection
δ_r	= rudder deflection
ϕ	= roll attitude
θ	= pitch attitude
$\dot{( )}$	= derivative with respect to time
$\underset{\sim}{( )}$	= transpose of a vector
$\underline{( )}$	= fast variables in slow-time scale
$( )$	= slow variables in fast-time scale

Presented as Paper 85-1890 at the AIAA Guidance and Control Conference, Snowmass, CO, Aug. 19-21, 1985; received Aug. 27, 1985; revision received April 16, 1986.

*Research Scientist. Member AIAA.
†Research Scientist.
‡Manager, Aircraft and Robotics Division. Member AIAA.
§Aerospace Engineer, OFDC. Member AIAA.

I. Introduction

THE motivation for the development of flight test trajectory controllers is well documented in the literature.[1-6] The primary objective is to enable the pilot to follow complex flight test trajectories consistently and accurately. Two versions of these controllers have been employed, viz., a closed-loop automatic system and an open-loop system providing manual piloting information. Originally, the open-loop flight test trajectory guidance algorithms were developed on-line in a piloted simulation using cut-and-dry techniques. This approach was not only manpower intensive, but often produced less than desirable controllers. Closed-loop system designs based on linearized aircraft models[4-6] required the generation of large amounts of numerical data to arrive at satisfactory designs. Further, gain scheduling was found to be essential for acceptable performance.

The present paper deals with the synthesis of nonlinear flight test trajectory controllers using the recent results in the prelinearizing transformation theory[7-15] and the singular perturbation theory.[16-19] The application of singular perturbation theory to this problem simplifies the linearizing transformation considerably, in addition to providing a consistent means for eliminating ignorable state variables. In this framework, the state variables in the original nonlinear problem are retained, while the control variables are transformed. This is advantageous from an implementation point of view. Splitting the dynamics based on the speed of state variable evolution generates a controller in which certain control loops can be computed at a slower rate than others on the flight control computer. In Ref. 9, it is interesting to note that, even though the controller development did not make use of singular perturbation theory, the time scale separation formed a basis for implementation on the flight control computer. Note, however, that the flight test trajectory control problem discussed here is distinct from those described in Refs. 7-10; in those investigations, the trajectory to be followed consisted of three position components specified as a function of time.

The flight test trajectory controller synthesis for a currently operational, fixed-wing high-performance fighter aircraft without VTOL or hover capabilities will be discussed in this paper. Although specific engine and airframe models are required for implementation, these will not be discussed since they are not central to the material to be presented. It will be assumed that the aircraft under consideration has the four usual controls: throttle, aileron, rudder, and elevator. It is further assumed that the aircraft has no direct force generation devices other than engine thrust without thrust vectoring capabilities. The task of the flight test trajectory controller is to track the given commands in airspeed, angle of attack, angle of sideslip, and altitude in the presence of disturbances and modeling uncertainties.

The next section will discuss the aircraft modeling and time-scale separation. The details of prelinearization and slow/fast controller synthesis will be given in Sec. III. Simulation results using the nonlinear flight test trajectory controllers will be presented in Sec. IV.

II. Modeling and Time-Scale Separation

The equations of motion for an aircraft flight over a flat, nonrotating Earth with zero ambient winds are given by[20]

$$\dot{V} = [-D\cos\beta + S\sin\beta + (k_1\cos\alpha\cos\beta + k_3\sin\alpha\cos\beta)T - mg(\sin\theta\cos\alpha\cos\beta - \cos\theta\sin\phi\sin\beta - \cos\theta\cos\phi\sin\alpha\cos\beta)]/m \quad (1)$$

$$\dot{\alpha} = [-L + (k_3\cos\alpha - k_1\sin\alpha)T + mg(\cos\theta\cos\phi\cos\alpha + \sin\theta\sin\alpha)]/mV\cos\beta + q - \tan\beta(p\cos\alpha + r\sin\alpha) \quad (2)$$

$$\dot{\beta} = [D\sin\beta + S\cos\beta - (k_1\cos\alpha\sin\beta + k_3\sin\alpha\sin\beta)T + mg \times (\sin\theta\cos\alpha\sin\beta + \cos\theta\sin\phi\cos\beta - \cos\theta\cos\phi \times \sin\alpha\sin\beta)]/Vm + p\sin\alpha - r\cos\alpha \quad (3)$$

$$\dot{h} = V(\cos\beta\cos\alpha\sin\theta - \sin\beta\sin\phi\cos\theta - \cos\beta\sin\alpha\cos\phi\cos\theta) \quad (4)$$

$$\dot{\phi} = p + q\sin\phi\tan\theta + r\cos\phi\tan\theta \quad (5)$$

$$\dot{\theta} = q\cos\phi - r\sin\phi \quad (6)$$

$$\epsilon\dot{P} = [PI_1 + RI_3 + e_1I_1\delta_a + e_2I_1\delta_q + e_3I_1\delta_r + pq(I_{xz}I_1 - D_zI_3) - qr(D_xI_1 + I_{xz}I_3)]/I \quad (7)$$

$$\epsilon\dot{q} = [QI_4 + f_1I_4\delta_e + f_2I_4\delta_a + f_3I_4\delta_r + pI_{xz}I_4 - prD_yI_4 + rI_{xz}I_4]/I \quad (8)$$

$$\epsilon\dot{r} = [PI_3 + RI_6 + g_1I_6\delta_e + g_2I_6\delta_a + g_3I_6\delta_r + pq(I_{xz}I_3 - D_zI_6) - qr(D_xI_3 + I_{xz}I_6]/I \quad (9)$$

where

$$I_1 = I_yI_z, \quad I_3 = I_yI_{xz}$$

$$I_4 = I_xI_z - I_{xz}^2, \quad I_6 = I_xI_y$$

$$D_x = I_z - I_y, \quad D_y = I_x - I_z$$

$$D_z = I_y - I_x, \quad I = I_xI_yI_x - I_yI_{xz}^2$$

$I_{xy} = I_{yz} = 0$ for the aircraft under consideration

The downrange x, the cross range y, and yaw attitude ψ are ignorable in the flight test trajectory problem under consideration. Consequently, the equations describing their dynamics have been eliminated. The interpolation parameter ϵ introduced on the left-hand sides of Eqs. (7-9) is motivated from the forced singular perturbation theory[19] and serves to indicate the difference in time scale between Eqs. (1-6) and the body rate Eqs. (7-9). Thus, with $\epsilon = 0$, one obtains the slow-time scale problem, while $\epsilon = 1$ yields the complete system. Assuming that the control surface deflections have a relatively small effect on lift, drag, and side force, with $\epsilon = 0$, the fast variables p, q, and r appear "control like" in the system [Eqs. (1-6)] with three nonlinear algebraic equations relating them to control surface deflections.

This approach runs into difficulty however, since Eq. (4) does not contain the p, q, and r components explicitly. To remedy this situation, Eq. (4) is differentiated once with respect to time; substituting for $\dot{\phi}$ and $\dot{\theta}$ from Eqs. (5) and (6), one then obtains

$$\dot{h} = H \quad (10)$$

$$\dot{H} = b_0\dot{V} + b_1\dot{\beta} + b_2\dot{\alpha} + a_0p + \alpha_1q + \alpha_2r \quad (11)$$

where

$$a_0 = b_4$$

$$a_1 = b_3\cos\phi + b_4\sin\phi\tan\theta$$

$$a_2 = b_4\cos\phi\tan\theta - b_3\sin\phi$$

and

$$b_0 = (\cos\beta\cos\alpha\sin\theta - \sin\beta\sin\phi\cos\theta - \cos\beta\sin\alpha\cos\phi\cos\theta)$$

$$b_1 = V(-\sin\beta\cos\alpha\sin\theta - \cos\beta\sin\phi\cos\theta + \sin\beta\sin\alpha\cos\phi\cos\theta)$$

$$b_2 = V(-\cos\beta\sin\alpha\sin\theta - \cos\beta\cos\alpha\cos\phi\cos\theta)$$

$$b_3 = V(\cos\beta\cos\alpha\cos\theta + \sin\beta\sin\phi\sin\theta + \cos\beta\sin\alpha\cos\phi\sin\theta)$$

$$b_4 = V(-\sin\beta\cos\phi\cos\theta + \cos\beta\sin\alpha\sin\phi\cos\theta)$$

In order to illustrate the singular perturbation procedure, the Eqs. (1-3) and (5-11) are next expressed in a compact form as

$$\dot{x} = A_1(x) + B_1(x)z + C_1(x)u_1 \quad (12)$$

$$\epsilon\dot{z} = A_2(x,u_1,z) + B_2(z) + C_2(x)u_2 \quad (13)$$

with

$$\underline{x} = [V,\alpha,\beta,\theta,\phi,h,H]$$

$$u_1 = T$$

$$\underline{z} = [pqr]$$

$$\underline{u}_2 = [\delta_e\delta_a\delta_r]$$

A nonlinear controller for the system of Eqs. (12) and (13) can be designed by transforming it into Brunovsky's canonical form.[12] But this would involve the computation of partial derivatives of the terms $A_1(x)$, $B_1(x)$, and $C_1(x)$.

This difficulty is avoided by invoking the assumption that the body rates p, q, and r evolve faster than other variables.

In the following, slow/fast controller synthesis using singular perturbation theory is discussed without any theoretical development. Setting $\epsilon=0$ in the system of Eqs. (12) and (13), one obtains the slow system as

$$\dot{x}=A_1(x)+B_1(x)z+C_1(x)u_1 \tag{14}$$

$$0=A_2(x,u_1,\bar{z})+B_2(\bar{z})+C_2(x)\bar{u}_2 \tag{15}$$

Here, $\bar{z}$ are the values of fast-state variables in the slow-time scale. Ideally, as in Ref. 16, one should solve for $\bar{z}$ in terms of $\bar{u}_2$ from Eq. (15) and substitute in Eq. (14) to obtain a system independent of $\bar{z}$. This is difficult in the aircraft trajectory control problem due to the nature of the functions A_2 and B_2. Alternatively, a nonlinear controller can be synthesized for the dynamic system of Eq. (14) with $\bar{z}$ and u_1 as the controls to track the required x commands. Next, the $\bar{z}$ obtained from this exercise can be substituted in Eq. (15) to solve for $\bar{u}_2$, provided that $C_2(x)$ is invertible. This completes the design of slow-time scale system.

To derive the fast-time scale controller, one assumes that the slow variables are constant in the fast-time scale dynamics. Subtracting Eq. (15) from Eq. (13) and putting

$$\Delta z=z-\bar{z},\ \Delta u=u_2-\bar{u}_2$$

one has

$$\Delta\dot{z}=A_3(\bar{x},\bar{u}_1,\Delta z)+B_3(\Delta z)+C_2(\bar{x})\Delta u \tag{16}$$

where $\bar{x}$ and $\bar{u}_1$ are values of slow state variables in the fast-time scale problem. A nonlinear feedback controller can again be designed for Eq. (16) to maintain Δz close to zero. As long as the body rate dynamics remain faster than other dynamics, one would expect a satisfactory performance from this controller. A time scale separation similar to the one discussed here has been employed in the past for flight control system design and is known to be valid in most situations. If the actuator dynamics are to be included in the control system synthesis, they can be handled in an additional time scale. Thus, with time scale separation, the flight test trajectory controller will be of the form given in Fig. 1.

In the present formulation, the engine dynamics is assumed to be faster than the airspeed dynamics. Although closed-loop thrust control is not attempted here, a first-order engine lag will be included during the controller evaluation.

In summary, the singular perturbation scheme described relies on the fact that the control surface deflections contribute relatively small forces on the airframe, a reasonable assumption for currently operational high-performance fighter aircraft.

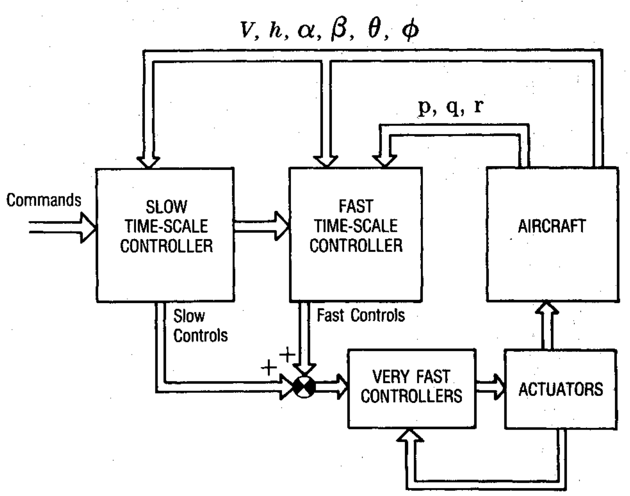

Fig. 1 SP nonlinear flight test trajectory controller.

III. Nonlinear Controller Design

The main specification on the flight test trajectory controller is that it should track given time histories of V, h, and α, While there are no direct specifications on the angle of sideslip β, it is desirable to maintain it close to zero throughout a given maneuver. In the following, the slow and fast-time scale controllers for tracking these variables will be discussed with specific details.

Slow-Time Scale Controller

Setting the interpolation parameter ϵ to zero, the slow-time scale dynamics given by Eqs. (1-3), (5), (6), (10), and (11) can be written as

$$\dot{V}=c_0+c_1T \tag{17}$$

where

$$c_0=[-D\cos\beta+S\sin\alpha-mg(\sin\theta\cos\alpha\cos\beta$$
$$-\cos\theta\sin\phi\sin\beta-\cos\theta\cos\phi\sin\alpha\cos\beta)]/m$$

$$c_1=(k_1\cos\alpha\cos\beta+k_3\sin\alpha\cos\beta)/m$$

$$\dot{\alpha}=c_2+c_3T+c_4\tilde{p}+c_5\tilde{q}+c_6\tilde{r} \tag{18}$$

where

$$c_2=[-L+mg(\cos\theta\cos\phi\cos\alpha+\sin\theta\sin\alpha)]/mV\cos\beta$$

$$c_3=(k_3\cos\alpha-k_1\sin\alpha)/mV\cos\beta$$

$$c_4=-\cos\alpha\tan\beta$$

$$c_5=1$$

$$c_6=-\tan\beta\sin\alpha$$

$$\dot{\beta}=d_0+d_2T+d_2\tilde{p}+d_3\tilde{r} \tag{19}$$

where

$$d_0=[D\sin\beta+S\cos\beta+mg(\sin\theta\cos\alpha\sin\beta$$
$$+\cos\theta\sin\phi\cos\beta-\cos\theta\cos\phi\sin\alpha\sin\beta)]/Vm$$

$$d_1=(-k_1\cos\alpha\sin\beta-k_3\sin\alpha\sin\beta)/Vm$$

$$d_2=\sin\alpha$$

$$d_3=-\cos\alpha$$

$$\dot{\phi}=d_4\tilde{p}+d_5\tilde{q}+d_6\tilde{r} \tag{20}$$

$$\dot{\theta}=d_7\tilde{q}+d_8\tilde{r} \tag{21}$$

where

$$d_4=1 \qquad d_7=\cos\phi$$

$$d_5=\sin\phi\tan\theta \qquad d_8=-\sin\phi$$

$$d_6=\cos\phi\tan\theta$$

$$\dot{h}=H \tag{22}$$

$$\dot{H}=b_0\dot{V}+b_1\dot{\beta}+b_2\dot{\alpha}+a_0\tilde{p}+a_1\tilde{q}+a_2\tilde{r} \tag{23}$$

$$0=[\tilde{P}I_1+\tilde{R}I_3+e_1I_1\tilde{\delta}_e+e_2I_1\tilde{\delta}_a+e_3I_1\tilde{\delta}_r$$
$$+\tilde{p}\tilde{q}(I_{xz}I_1-D_zI_3)-\tilde{q}\tilde{r}(D_xI_1+I_{xz}I_3)]/I \tag{24}$$

$$0=[\tilde{Q}I_4+f_1I_4\tilde{\delta}_e+f_2I_4\tilde{\delta}_a+f_3I_4\tilde{\delta}_r+\tilde{p}^2I_{xz}I_4$$
$$-\tilde{p}\tilde{r}D_yI_4+\tilde{r}^2I_{xz}I_4]/I \tag{25}$$

$$0=[\tilde{P}I_3+\tilde{R}I_6+g_1I_6\tilde{\delta}_e+g_2I_6\tilde{\delta}_a+g_3I_6\tilde{\delta}_r$$
$$+\tilde{p}\tilde{q}(I_{xz}I_3-D_zI_6)-\tilde{q}\tilde{r}(D_xI_3+I_{xz}I_6)]/I \tag{26}$$

Equations (17-26) describe the slow-time scale dynamics with control variables $\tilde{p},\tilde{q},\tilde{r}$, and T, the body rates, and the engine thrust. Since there are seven state variables and four control variables, only four of these states can be completely controlled.

The variables of interest in the present flight test trajectory control problem can be grouped into two sets, i.e., 1) V, h, α,β or 2) V, h,β,ϕ, either of which can be tracked by the trajectory controller. Consequently, the number of states to be controlled is equal to the number of controls. The other state variables are treated as free. The discussions in the following will be limited to case 1. Case 2 can be handled in an entirely analogous manner. Since there are four state variables to be tracked and four control variables, the slow-time scale system can be put in the following form by defining four new pseudocontrols U_1, U_2, U_3, and U_4:

$$\dot{h}=H \qquad \dot{\alpha}=U_3$$
$$\dot{H}=U_1 \qquad \dot{\beta}=U_4$$
$$\dot{V}=U_2 \tag{27}$$

Next, four independent linear controllers can be designed for this system to ensure zero tracking errors for ramp commands. Typically, the airspeed, angle of attack, and angle of side slip will have proportional plus integral control, while the altitude loop will have a proportional plus deriviative control. The forms of these pseudocontroller loops are given in Fig. 2. If desired, an integral feedback may be incorporated in the altitude channel to improve the tracking response. However, this was not found necessary for the maneuvers considered in the present work.

It can be verified that, except for the altitude loop, all other controllers will have zero steady-state errors for the ramp commands. Moreover, the natural frequencies and damping ratios of these control loops are as follows:

1) Airspeed loop:

$$\omega_{n_V}=\sqrt{k_2}, \qquad \xi_V=k_1/2\sqrt{k_2}$$

2) Angle-of-attack loop:

$$\omega_{n_\alpha}=\sqrt{k_4}, \qquad \xi_\alpha=k_3/2\sqrt{k_4}$$

3) Angle of sideslip:

$$\omega_{n_\beta}=\sqrt{k_6}, \qquad \xi_\beta=k_5/2\sqrt{k_6}$$

4) Altitude loop:

$$\omega_{n_h}=\sqrt{k_7}, \qquad \xi_h=\sqrt{k_7k_8}/2$$

Hence, two time response specifications can be set for each of these control loops. Note, however, that the extent to which these specifications are met will depend on the actuator saturation levels and the tracking commands.

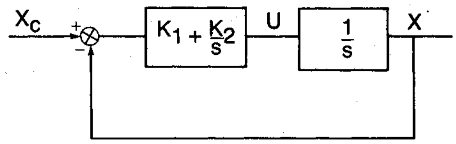

a) Airspeed, angle of attack, and angle of sideslip loops ($X=V$, α, or β).

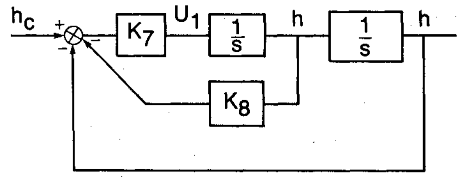

b) Altitude control loop.

Fig. 2 Structure of the pseudocontrol loops.

The remaining task in the slow-time scale control problem is that of converting the four pseudocontrols into the four real controls. Thus, from Eqs. (17-19) and (23), one has

$$T=(U_2-c_0)/c_1 \tag{28}$$

$$\begin{bmatrix} a_0 & a_1 & a_2 \\ c_4 & c_5 & c_6 \\ d_2 & 0 & d_3 \end{bmatrix}\begin{bmatrix}\tilde{p}\\ \tilde{q}\\ \tilde{r}\end{bmatrix}=\begin{bmatrix} U_1-(b_0U_2+b_1U_4+b_2U_3) \\ U_3-c_2-c_3T \\ U_4-d_0-d_1T \end{bmatrix} \tag{29}$$

It is assumed here that the required thrust given by Eq. (28) can be converted into the corresponding throttle setting using tabular data. The set of linear Eqs. (29) can be solved for $\tilde{p}$, $\tilde{q}$, and $\tilde{r}$. If the aircraft is in symmetric flight, the 3×3 matrix premultiplying the $\tilde{p}$, $\tilde{q}$, $\tilde{r}$ vector will have a rank less than three. This is because under these conditions, in the reduced-order problem, there are three longitudinal state variables to be controlled, while there are only two available controls, viz. the thrust T and the pitch body rate $\tilde{q}$. Hence, one can precisely control the airspeed and altitude, or the airspeed and angle of attack, or the angle of attack and altitude. However, if a linear combination of any two of these three variables is formed, then that linear combination can be controlled exactly along with the remaining variable. The situation in the lateral channel is opposite under the symmetric flight conditions, i.e., there are two control variables, $\tilde{r}$ and $\tilde{p}$ available, while there is just one state $\tilde{\beta}$ to be controlled. Thus, in the lateral channel, the angle of side slip can be maintained zero either by the yaw body rate $\tilde{r}$ or the roll body rate $\tilde{p}$ or by a linear combination of these. The approach adopted in the present work is to use $\tilde{r}$ to control $\tilde{\beta}$, while using $\tilde{p}$ to maintain the roll attitude at zero when the aircraft is in symmetric flight.

Once the Eqs. (28) and (29) have been solved, the $\tilde{p}$, $\tilde{q}$, $\tilde{r}$ values and thrust can be substituted in Eqs. (24-26) to compute the control surface deflections $\tilde{\delta}_e$, $\tilde{\delta}_a$, $\tilde{\delta}_r$ along the "outer" solution.

Fast-Time Scale Controller

In the fast-time scale, the slow-time scale variables h, V, α, and β are assumed to remain constant. The fast-time scale controller attempts to maintain the body rates p, q, r close to their values in the "outer" solution. Subtracting Eqs. (24-26) from Eqs. (7-9) and putting

$$\Delta p=p-\tilde{p}, \quad \Delta q=q-\tilde{q}, \quad \Delta r=r-\tilde{r}$$

one obtains

$$\Delta\dot{p} = [(P-\tilde{P})I_1 + (R-\tilde{R})I_3 + e_1 I_1(\delta_e-\tilde{\delta}_e) + e_2 I_1(\delta_a-\tilde{\delta}_a) + e_3 I_1(\delta_r-\tilde{\delta}_r) + (\Delta p\cdot\Delta q + \tilde{p}\cdot\Delta q + \tilde{q}\cdot\Delta p)(I_{xz}I_1 - D_z I_3) - (\Delta q\cdot\Delta r + \tilde{q}\cdot\Delta r + \tilde{r}\cdot\Delta q)(D_x I_1 + I_{xz}I_3)]/I \qquad (30)$$

$$\Delta\dot{q} = [(Q-\tilde{Q})I_4 + f_1 I_4(\delta_e-\tilde{\delta}_e) + f_2 I_4(\delta_a-\tilde{\delta}_a) + f_3 I_4(\delta_r-\tilde{\delta}_r) + (\Delta p^2 + \Delta p\cdot\tilde{p})I_{xz}I_4 - (\Delta p\cdot\Delta r + \Delta r\cdot\tilde{p} + \Delta p\cdot\tilde{r})D_y I_4 + (\Delta r^2 + \Delta r\cdot\tilde{r})I_{xz}I_4]/I \qquad (31)$$

$$\Delta\dot{r} = [(P-\tilde{P})I_3 + (R-\tilde{R})I_6 + g_1 I_6(\delta_e-\tilde{\delta}_e) + g_2 I_6(\delta_a-\tilde{\delta}_a) + g_3 I_6(\delta_r-\tilde{\delta}_r) - (\Delta p\cdot\Delta r + \tilde{q}\cdot\Delta r + \tilde{r}\cdot\Delta q)(D_x I_3 + I_{xz}I_6)]/I \qquad (32)$$

The fast-time scale controller maintains Δp, Δq, and Δr close to zero throughout a given maneuver. Since there are three independent controls available, three pseudocontrols are next defined such that the system of Eqs. (30-32) takes the form

$$\Delta\dot{p} = U_5, \quad \Delta\dot{q} = U_6, \quad \Delta\dot{r} = U_7 \qquad (33)$$

Three independent control loops can be designed in pseudocontrols U_5, U_6, and U_7 such that Eq. (33) has a much faster time constant than the slow-time scale system of Eqs. (17-26). Integral feedbacks are not necessary for these control loops, since there are no explicit tracking requirements. The real controls can be obtained from pseudocontrols using

$$\begin{bmatrix} e_1 I_1 & e_2 I_1 & e_3 I_1 \\ f_1 I_4 & f_2 I_4 & f_3 I_4 \\ g_1 I_6 & g_2 I_6 & g_3 I_4 \end{bmatrix} \begin{bmatrix} (\delta_e-\tilde{\delta}_e) \\ (\delta_a-\tilde{\delta}_a) \\ (\delta_r-\tilde{\delta}_r) \end{bmatrix} = \begin{bmatrix} f_4 \\ f_5 \\ f_6 \end{bmatrix} \qquad (34)$$

where

$$f_4 = IU_5 - (P-\tilde{P})I_1 - (R-\tilde{R})I_3 - (\Delta p\cdot\Delta q + \tilde{p}\cdot\Delta q + \tilde{q}\cdot\Delta p) \times (I_{xz}I_3 - D_z I_6) - (\Delta q\cdot\Delta r + \tilde{q}\cdot\Delta + r\tilde{r}\cdot\Delta q) \times (D_x I_1 + I_{xz}I_3)$$

$$f_5 = IU_6 - (Q-\tilde{Q})I_4 - (\Delta p^2 + \Delta p\cdot\tilde{p})I_{xz}I_4 + (\Delta p\cdot\Delta r + \Delta r\cdot\tilde{p} + \Delta\cdot p\tilde{r})D_y I_4 - (\Delta r^2 + \Delta r\cdot\tilde{r})I_{xz}I_4$$

$$f_6 = IU_7 - (P-\tilde{P})I_3 - (R-\tilde{R})I_6 + (\Delta q\cdot\Delta r + \tilde{q}\cdot\Delta r + \tilde{r}\cdot\Delta q) \times (D_x I_3 + I_{xz}I_6)$$

The set of linear algebraic equations (34) can be solved for $(\delta_e-\tilde{\delta}_e)$, $(\delta_a-\tilde{\delta}_a)$, and $(\delta_r-\tilde{\delta}_r)$. Note that the matrix multiplying these quantities has full rank everywhere on the flight envelope and a unique solution always exists. Since $\tilde{\delta}_e$, $\tilde{\delta}_a$, $\tilde{\delta}_r$ are known from the outer solution, the actual control surface deflections can be computed.

IV. Nonlinear Controller Evaluation

In order to test the performance of the nonlinear controller synthesized in the previous section, it is implemented on a six-degrees-of-freedom simulation of a high-performance fighter aircraft including first-order engine dynamics. Two symmetric flight test maneuvers will be illustrated here, viz., a level acceleration trajectory and a pushover/pullup trajectory.

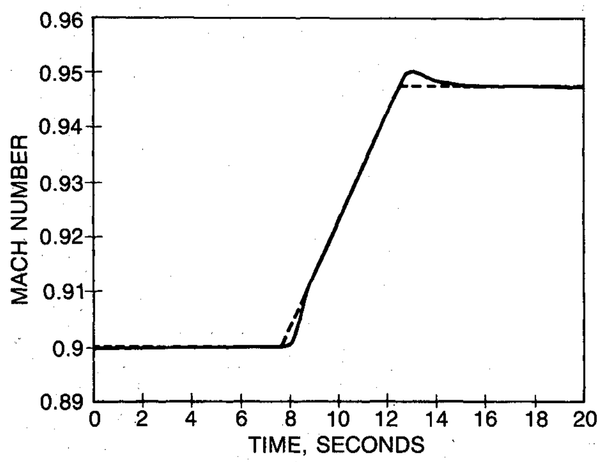

Fig. 3 Mach number evolution along the level acceleration flight test trajectory (dotted line denotes the commanded Mach number and solid line the actual Mach number).

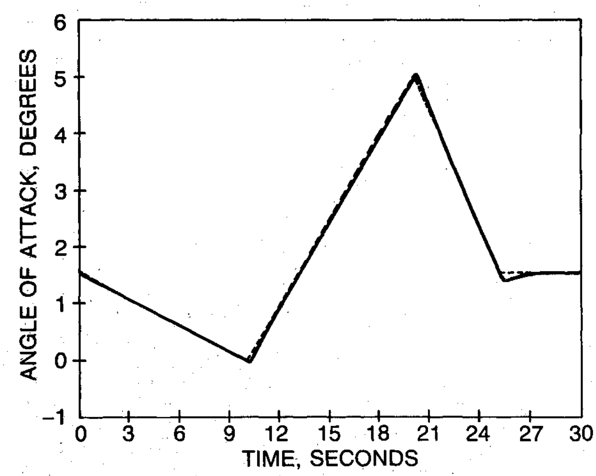

Fig. 4 Angle of attack along the pushover/pullup flight test trajectory (dotted line denotes the commanded angle of attack and solid line the actual angle of attack).

The level acceleration trajectory is a wings-level, constant-altitude maneuver with a ramp Mach number command. This maneuver is initiated at 20,000 ft and Mach 0.9. The objective is to accelerate the aircraft at about 10 ft/s^2 for 5 s. An initial constant Mach number leg is included in the command history to provide adequate time for damping out the effect of inexact trim conditions. The Mach number command as well as the aircraft response are given in Fig. 3. The Mach number tracking error is less than ± 0.001 during most of the acceleration phase. The altitude is maintained with ± 0.2 ft throughout the maneuver.

A pushover/pullup trajectory is executed next. This flight test trajectory is a wings/level, constant Mach number maneuver in which the angle of attack is varied a specified increment about the trim value at some specified rate. Figure 4 depicts the commanded and the actual angle of attack. The angle-of-attack tracking error is well within ± 0.1 deg. The Mach number was maintained within ± 0.006 throughout the maneuver, as can be observed from Fig. 5. A transient appearing at 20 s in the Mach number history is due to the throttle thrust characteristics of the engine. For this aircraft engine, there is a small core thrust saturation region approximately between 83 and 98 deg of throttle setting. Note that, in this maneuver, the altitude is not controlled and is therefore free to change as it may throughout the trajectory. The resulting altitude history is given in Fig. 6. During the initial negative angle-of-attack rate region (as well as for some positive angle-

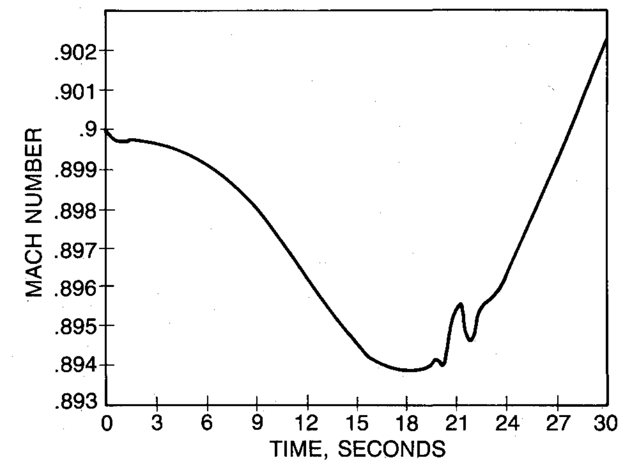

Fig. 5 Mach number evolution along the pushover/pullup flight test trajectory.

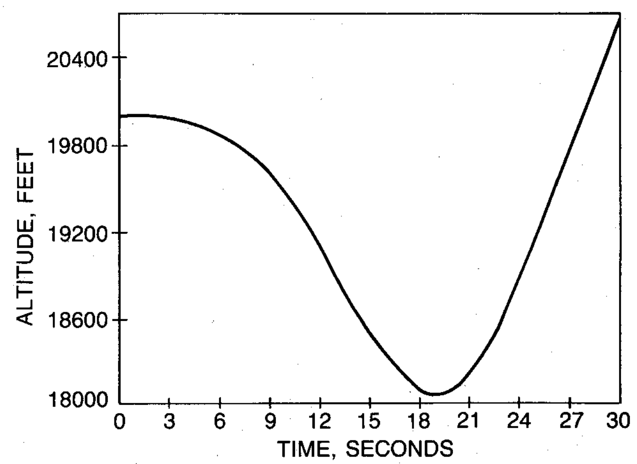

Fig. 6 Altitude evolution along the pushover/pullup flight test trajectory.

of-attack rate), the aircraft loses as much as 2000 ft. During the second half of this manevuer, the aircraft gains altitude and overshoots the intial altitude by almost 600 ft. If desired, the command angle-of-attack history can be tailored to return the aircraft to initial straight and level conditions at the end of the maneuver.

Summarizing the results presented so far, the nonlinear controller performance for these two maneuvers has been found very good. The controller performance and several other maneuvers have been evaluated with equally satisfactory results. These controllers are currently being implemented on a manned simulation as a first step toward flight testing.

V. Conclusions

Nonlinear controllers for tracking flight test trajectory commands were described. The controller development employed singular perturbation theory and the recent prelinearizing transformation results for a class of nonlinear systems. The synthesized controllers do not require gain scheduling and can be implemented at different rates on the flight control computer. The approach presented here can be extended fortrack-ing three positions components and velocity, for example, as in an autoland task. The synthesized control laws have a general character in the sense that their form remains invariant for any conventional aircraft. However, the time scale separation presented must be valid for the maneuver under consideration.

Acknowledgments

The first author would like to thank Dr. George Meyer of NASA Ames Research Center for kindly furnishing us with the copies of his papers and reports. We thank Mr. Robert Antoniewicz of NASA Ames-Dryden Flight Research Facility for help in the controller implementation.

This research was suported by NASA Ames-Dryden Flight Research Facility under Contract NAS2-11877.

References

[1]Duke, E.L., "Automated Flight Test Maneuvers: The Development of a New Technique," *Flight Testing Technology: A State-of-the-Art Review, Proceedings of the Society of Flight Test Engineers 13th Annual Symposium,* New York, Sept. 1982, pp. 101-119.

[2]Duke, E.L., Swann, M.R., Enevoldson, E.K., and Wolf, T.D., "Experience with Flight Test Trajectory Guidance," *Journal of Guidance, Control, and Dynamics,* Vol. 6, Sept.-Oct. 1983, pp. 393-398.

[3]"Final Report, HiMAT Maneuver Autopilot," Teledyne Ryan, Aero. Rept. TRA 29255-1, Feb. 1981.

[4]Walker, R.A. and Gupta, N.K., "Flight Test Trajectory Control Analysis," NASA CR 170395, Feb. 1983.

[5]Menon, P.K.A., Saberi, H.A., Walker, R.A., and Duke, E.L., "Flight Test Trajectory Controller Synthesis with Eigenstructure Assignment," *Proceedings of 1985 American Control Conference, IEEE,* June 1985, pp. 1181-1186.

[6]Menon, P.K.A. and Walker, R.A., "Aircraft Flight Test Trajectory Control," Integrated Systems, Inc., Palo Alto, CA, Rept. 56 prepared for NASA Ames-Dryden Flight Research Facility under Contract NAS2-11877, March 1985.

[7]Meyer, G. and Cicolani, S., "A Formal Structure for Advanced Automatic Flight Control Systems," NASA TN D-7940, 1975.

[8]Brockett, R.W., "Nonlinear Systems and Differential Geometry," *Proceedings of the IEEE,* Vol. 64, Feb. 1976, pp. 61-72.

[9]Smith, G.A. and Meyer, G., "Total Aircraft Flight-Control System—Balanced Open- and Closed-Loop Control with Dynamic Trim Maps," *Proceedings of Third Digital Avionics Systems Conference,* No. 79CH1518-0, IEEE, New York, Nov. 1979.

[10]Smith, G.A. and Meyer, G., "Application of the Concept of Dynamic Trim Control to Automatic Landing of Carrier Aircraft," NASA TP-1512, 1980.

[11]Hunt, L.R., and Su, R., "Control of Nonlinear Time-Varying Systems," *Proceedings of IEEE Conference on Decision and Control,* IEEE, New York, 1981, pp. 558-563.

[12]Hunt, L.R., Su, R., and Meyer, G., "Global Transformations of Nonlinear Systems," *IEEE Transactions on Automatic Control,* Vol. AC-28, Jan. 1983, pp. 24-31.

[13]Hunt, L.R., Su, R., and Meyer, G., "Multi-Input Nonlinear Systems," *Differential Geometric Control Theory Conference,* Birkhauser, Boston, 1982.

[14]Meyer, G., Su, R., and Hunt, L.R., "Application of Nonlinear Transformations to Automatic Flight Control," *Automatica,* Vol. 20, 1984, pp. 103-107.

[15]Dwyer, T.A.W., "Exact Nonlinear Control of Large Angle Rotational Maneuvers," *IEEE Transactions Automatic Control,* Vol. AC-29, Sept. 1984, pp. 769-774.

[16]Chow, J.H. and Kokotovic, P.V., "Two-Time-Scale Feedback Design of a Class of Nonlinear Systems," *IEEE Transactions on Automatic Control,* Vol. AC-23, June 1978, pp. 438-443.

[17]Chow, J.H. and Kokotovic, P.V., "A Decomposition of Near-Optimum Regulators for Systems with Slow and Fast Modes," *IEEE Transaction on Automatic Control,* Vol. 21, Oct. 1976, pp. 701-705.

[18]Khalil, H.K., "Linear Quadratic Gaussian Estimation and Control of Singularly Perturbed Systems," *Singular Perturbations in Systems and Control,* CISM Courses and Lectures 280, edited by M.D. Ardema, Springer-Verlag, Vienna and New York, 1984.

[19]Kelley, H.J., "Aircraft Maneuver Optimization by Reduced Order Approximation," *Control and Dynamic Systems,* Vol. 10, edited by C.T. Leondes, Academic Press, New York, 1973, pp. 131-178.

[20]Etkin, B., *Dynamics of Atmospheric Flight,* John Wiley & Sons, New York, 1972.